AUTOMATIC APPROACH FOR RECTIFYING BUILDING FACADES FROM A SINGLE UNCALIBRATED IMAGE

Wenting Duan and Nigel M. Allinson
The Department of Electronic and Electrical Engineering, The University of Sheffield
Mappin Street, Sheffield, U.K.

Keywords: Facade rectification, Vanishing point estimation, Line grouping, Building recognition.

Abstract: We describe a robust method for automatically rectifying the main facades of buildings from single images taken from short to medium distances. This utility is an important step in building recognition, photogrammetry and other 3D reconstruction applications. Our main contribution lies in a refinement technique for vanishing point estimation and building line grouping, since both significantly affect the location and warping of building facades. The method has been shown to work successfully on 96% of images from the Zubud-Zurich building database where images frequently contain occlusions, different illumination conditions and wide variations in viewpoint.

1 INTRODUCTION

The rectification of main building facades to their fronto-parallel view is of importance in building recognition, photogrammetry and other 3D reconstruction applications (Wang et al., 2005). It can simplify the extraction of metric information and recover the canonical shape of a building because the metric rectification allows the scene to be warped-back using a similarity transformation. In other words, the rectified view is almost free from perspective distortion. It should be noted that the rectification problem addressed here is different from image rectification for stereo vision, where the purpose is to match the epipolar projections of image pairs (Hartley, 1999). How to rectify a single uncalibrated image is a different challenge; and various approaches having been proposed and studied.

As pointed out by Menudet et al. (2008), "camera self-calibration is intrinsically related to metric reconstruction". Therefore, an important factor for rectification lies in obtaining accurate calibration parameters and inclusion of appropriate scene constraints. Menudet et al. (2008) described a new way of decomposing the scene-to-image homography, which allows a cost function to assess how close the rectification is to similarity. However, to obtain the calibration parameters, at least four images of the same scene were required. Using only a single image of a particular scene, Liebowits and Zisserman (1998) utilised some geometric constraints such as equal angles for rectification. Chen and Ip (2005) achieved rectification by using the vanishing line and an arbitrary circle extracted from the image to estimate the image of the absolute conic (IAC). In the context of rectifying building images, reliable geometric features such as parallel lines and orthogonal angles can be used as scene constraints (Hu, Sawyer and Herve, 2006; Robertson and Cipolla, 2004; David, 2008; Košecká and Zhang, 2005). The estimation of the vanishing line is a major technique to recover images from perspective distortion. Hence, improving the accuracy and efficiency of computing these vanishing points is of foremost interest. Košecká and Zhang (2002) proposed a technique of applying the EM algorithm to detect vanishing points for images taken in man-made environments. The method achieved good accuracy with vanishing points being detected, on average, within 5 pixels of their true position. However, for building facade rectification, the following factors can adversely affect the success rate of detecting vanishing points. Firstly the images of the building can be taken in different illumination conditions and from different viewpoints. Secondly occlusion and scene clutter can obscure the building image. Finally, not all buildings have facades that are orthogonal to each other. These issues have not

Duan W. and Allinson N. (2009).
AUTOMATIC APPROACH FOR RECTIFYING BUILDING FACADES FROM A SINGLE UNCALIBRATED IMAGE.
In *Proceedings of the 6th International Conference on Informatics in Control, Automation and Robotics - Robotics and Automation*, pages 37-43
DOI: 10.5220/0002191600370043
Copyright © SciTePress

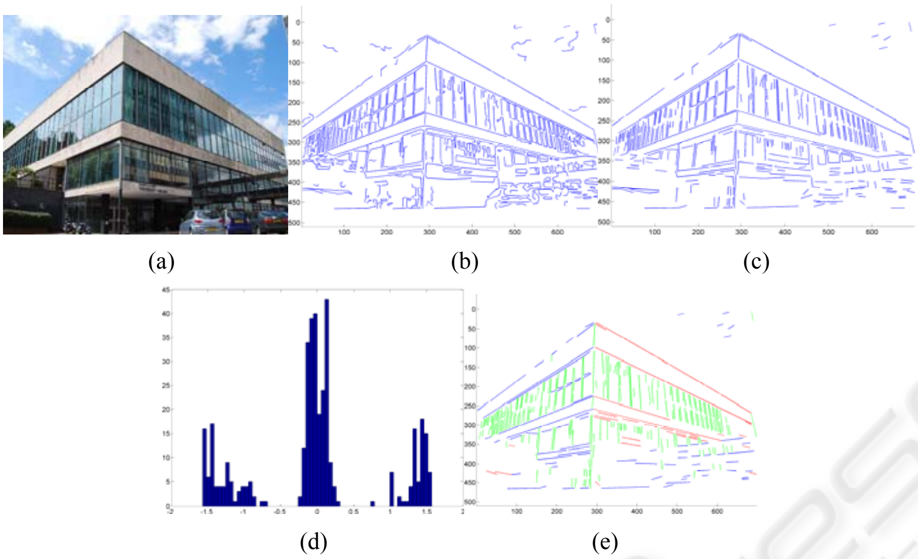

Figure 1: (a) Original Image (700×468 pixels) – Main Library of Sheffield University; (b) Line segments fitted to the connected edge points; (c) Line segments with length > 15 selected; (d) Histogram of line segment directions; (e) Separated groups of line segments associated with the three principal directions.

been considered by existing methods for building rectification, and for this reason it is desirable to develop more robust methods that can handle these potential problems.

In this paper, we first present a method based on Expectation-Maximisation (EM) algorithm for estimating the vanishing points of building images. Then, we show how to use the appropriate scene constraints appeared in the image to enable automatic rectification of the main building facades. The approach is described in Section 2. In Section 3, the results are presented and compared to Košecká and Zhang's work (2002). Finally, we draw some conclusions.

2 METHOD

2.1 Line Segments Detection and Initial Grouping

Lines, derived from local intensity edges, in building images contain significant and stable geometric information because the majority are aligned to the three principal axes. These three axes are associated with the 3D orthogonal real-world axes. Under perspective transformation, the parallel lines of buildings intersect at vanishing points in the image (though the actual vanishing points may be outside the area of the captured scene). Hence, first of all, we need to find those groups of lines that are associated with these vanishing directions. A conventional Canny edge detector was used to find edge strength and orientation followed by non-maximum suppression. Hysteresis thresholding was then used to further refine the recovered edges. We applied the edge-linking function (Kovesi, 2000-2006) to the detected edges to label connected edge points. The linked points with a length under 15 pixels were discarded since these lengths were determined experimentally to be inconsequential for our image sizes (typically 700×468 pixels). A line-fitting scheme was then utilised to form straight line segments from these linked edges. At this stage, a line segment list was produced, which contains the end point coordinates of all the computed line segments in the image coordinate frame. A typical example is shown in Fig. 1(b).

In Fig. 1(b), we can easily see that most short line segments belong to the background or general scene clutter. The many short ones belonging to the building are also not reliable. Hence, the length of each segment was calculated and again ones longer than 15 pixels were selected. This small step also enables us to roughly segment the building region from the whole scene (Fig. 1(c)). The directions of all the lines were calculated in order to compute the histogram shown in Fig. 1(d). The top peaks which are at least five bins apart were selected after curve fitting to the histogram. The lines which have orientation within the range of +/-π/8 around a particular peak were included in the same group.

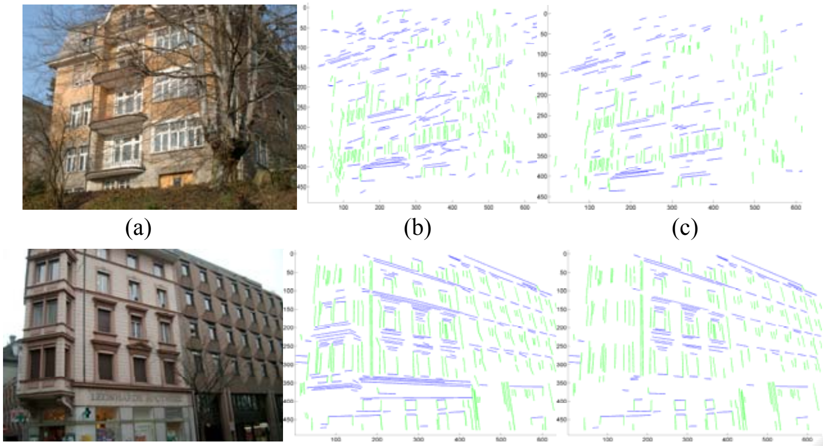

(a) (b) (c)

(d) (e) (f)

Figure 2: (a) Building with occlusion; (b) Detected and initially grouped two sets of lines for image (a); (c) Refined line groups for (a); (d) Building with confusing line directions; (e) Two initial groups of lines for image (d) – left side of the image contain lines that do not belong to the expected vanishing direction; (f) Refined line groups of (d).

The resultant three main groups are shown in Fig. 1(e) as separate colours.

For each group of line segments, we can now compute their initial vanishing point. In Fig. 1(e), each line segment is plotted by connecting their two end points $\mathbf{x_1}$ and $\mathbf{x_2}$. In a homogeneous form, $\mathbf{x_1} = (x_1,y_1,1)$ and $\mathbf{x_2} = (x_2,y_2,1)$. Under the 2D projective plane, the homogeneous line representation is obtained by:

$$\mathbf{l} = \mathbf{x_1} \times \mathbf{x_2} \tag{1}$$

As mentioned above, under perspective transformations, parallel lines in the real-world coordinate frame intersect at vanishing points in the image plane. The two lines $\mathbf{l_1}$ and $\mathbf{l_2}$ intersect at the point $\mathbf{v} = \mathbf{l_1} \times \mathbf{l_2}$. Alternatively, the relationship between vanishing points and their associated lines can be expressed as $\mathbf{v}^T\mathbf{l} = 0$. However, with so many pairs of lines available in each principal axis, we can produce many differing vanishing points. This requires us to solve the linear least square estimation problem:

$$\min_v \sum_{i=1}^{n} \left(l_i^T v\right)^2 \tag{2}$$

where n is the number of lines. This formula (2) can be written as

$$\min_{\mathbf{v}} \|\mathbf{Av}\|^2 \tag{3}$$

The rows of matrix $\mathbf{A}$ are the grouped lines with the same vanishing direction.

Before solving the linear least square estimation problem, we need to normalise the image end-point coordinates since we are dealing with the case of an uncalibrated camera. More detailed information of normalisation can be found in Košecká and Zhang (2002). The initial vanishing point for each group was calculated by the closed form solution of (3), where the estimation of $\mathbf{v}$ was the eigenvector associated with the smallest eigenvalue of $\mathbf{A}^T\mathbf{A}$. The initial grouping of lines and estimated vanishing points are accurate enough for the example image in Fig. 1(a). However, for images with occlusions or false groupings such as in Fig. 2(a) and (b), further refinement is necessary. For example, Fig. 2(a) shows a building with some occlusions. Its initial grouped lines (as shown in Fig. 2(b)) causes large errors in vanishing point detection. The building in Fig. 2(d) also contains lines that do not belong to the dominant vanishing directions but are still grouped.

2.2 Further Refinement of Vanishing Points Locations based on EM Algorithm

The refinement method is based on the Expectation Maximisation (EM) algorithm. We first compute the likelihood of line segments $\boldsymbol{l_i}$ belonging to each of the initially estimated vanishing points $\boldsymbol{v_k}$ by the formula:

$$p(l_i \mid v_k) \propto \exp\left(\frac{-\left(l_i^T v_k\right)^2}{2\sigma_1^2}\right) \tag{4}$$

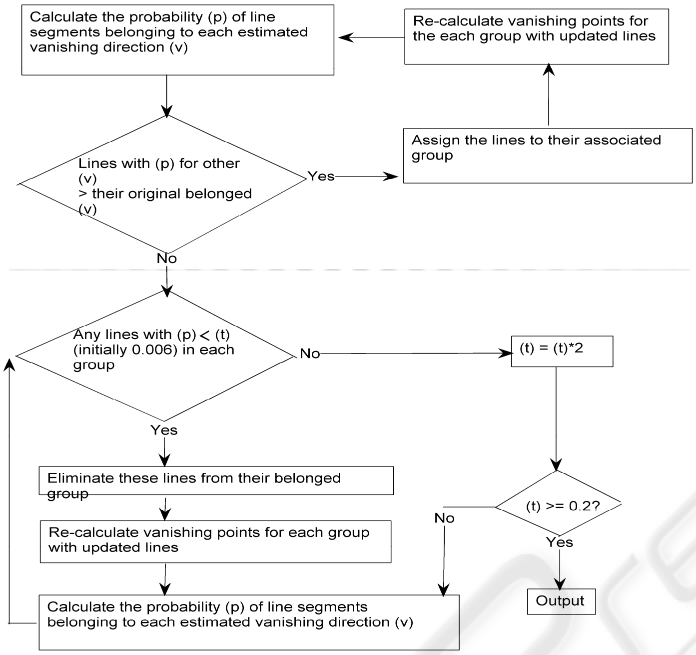

Figure 3: Flow chart of the refining process.

The upper half of the flow chart - Fig. 3 is mainly used for re-grouping lines and combining similar vanishing directions. The probabilities for each line corresponded to every vanishing direction were compared. The updated line groups were passed to the lower half of the algorithm when no lines are found to belong to other directions. The lower half eliminates lines with low probability for the direction they belong to so producing more accurate estimates of vanishing point locations. The iteration stops when line probabilities for each group are all above 0.1. In our experiments, t = 0.1 normally is sufficient to give an accurate vanishing point. The effect of this refining process for Fig. 2(a) and (d) is shown in Fig.2(c) and (f).

2.3 Automatic Rectification of Main Building Facades

To automatically warp an image's main building facades to the fronto-parallel view, we have to use the geometric information provided by the image, no external interaction should be required during the processing. We followed the approach described by Liebowitz and Zisserman (1998) as well as Hartley and Zisserman （2003). Here, we briefly summarize the method. The homography $\boldsymbol{H}$ which relates the points $\boldsymbol{x}$ in the image plane to $\boldsymbol{x'}$ （homogeneous 3-vector ） in the real-world plane can be decomposed into three transformation matrices: **H = Similarity * Affine * Projective**.

The first transformation is a pure projective transformation obtained with the vanishing line of the plane:

$$P = \begin{bmatrix} 1 & 0 & 0 \\ 0 & 1 & 0 \\ l_1 & l_2 & l_3 \end{bmatrix} \tag{5}$$

where l_1, l_2 and l_3 are the vector elements of the vanishing line $\boldsymbol{l}_\infty$. Since the vanishing line is computed by the two vanishing points from their corresponding facade, the vanishing point corresponds to the vertical lines of the building normally need to be used twice. For images with three vanishing points, we decided the vertical vanishing point by exploiting the location of the coordinates of all vanishing points with respect to the image's principal point.

The affine transformation which enables the recovery of metric geometry is expressed as:

$$A = \begin{pmatrix} \frac{1}{\beta} & -\frac{\alpha}{\beta} & 0 \\ 0 & 1 & 0 \\ 0 & 0 & 1 \end{pmatrix} \tag{6}$$

where α and β are the two parameters involved in the transformation of circular points from the metric plane to the affine plane. When the metric geometry is restored it includes angles and length ratios of

SCITEPRESS Science and Technology Publications

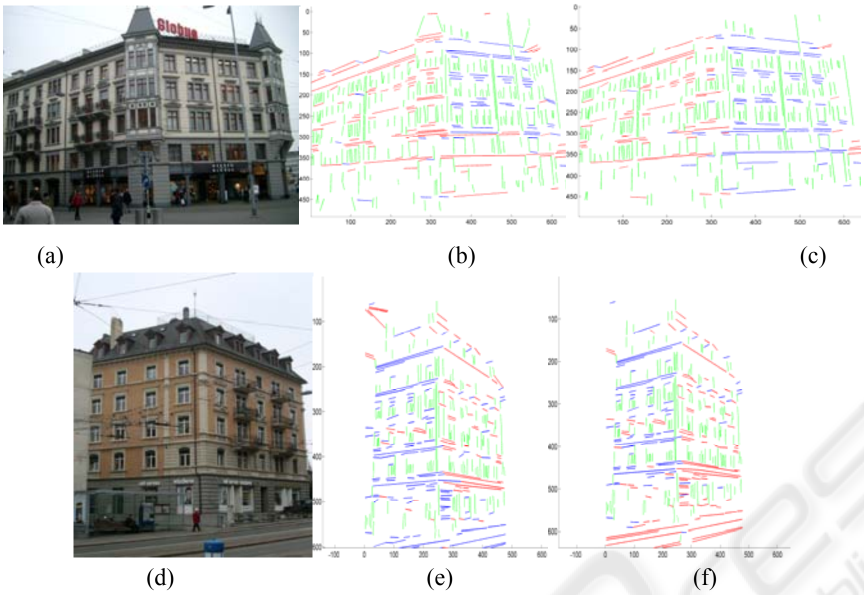

Figure 4: (a) Building with facades not aligned with the three orthogonal axes; (b) Initial grouping for image (a); (c) Refined line groups for (b); (d) Image taken from a critical viewpoint; (e) Plenty of lines grouped falsely; (f) Refined line groups for (e).

non-parallel line segments. In order to determine α and β, two constraints for non-parallel line sets must be supplied. The constraints can be obtained from “a known angle between lines; Equality of two (unknown) angles; and a known length ratio” (Liebowitz and Zisserman, 1998). Each constraint produces a circle in the complex plane with α and β indeed its real and imaginary components. The value of α and β can be found at the intersection points of two circles. However, for the problem of building facade rectification, there is only one constraint that the detected line segments provide with high confidence — the right angle between the two sets of lines. Therefore, the parameter β is assumed to be 1. This assumption is based on the fact that under affine transformations, the circular points with coordinates $(1,\pm i,0)^T$ in the metric plane are mapped to $(\alpha \mp i\beta,1,0)^T$. If no affine distortion occurred, the value of α and β is $(0, 1)^T$.

The last similarity transformation matrix is in the form of:

$$s = \begin{pmatrix} sR & t \\ 0^T & 1 \end{pmatrix} \quad \text{and} \quad R = \begin{pmatrix} \cos\theta & \sin\theta \\ -\sin\theta & \cos\theta \end{pmatrix} \qquad (7)$$

This final stage is used to: (i) adjust the image centre so that no coordinates of the image points has a negative value; (ii) rotate the line sets in order to make sure the majority of the lines in each group are aligned with the x and y axis directions; and (iii) scale the image up or down if the warped image size exceeds our desired value.

3 DISCUSSION

The approach proposed for building facade rectification was tested on the buildings images from the Zubud-Zurich buildings database (Shao and Gool, 2003). The method managed to rectify 96% of all the images tested. From this test, we found that the key to properly warp the building facades lies in the accuracy of the vanishing points and grouping of real-world parallel lines. The proposed refinement method was compared with Košecká and Zhang’s (2002) work on vanishing points detection. Our experiment shows following improvement in the context of rectifying building images:

(1) Accuracy of Estimated Vanishing Points. Instead of assigning probability weights to each line for the Maximisation step described in [11], the lines with very low probability to the vanishing point of the associated group are eliminated or assigned to other groups. Therefore, lines which could degrade the estimate of vanishing point are reduced. From our experiments, the average deviation of vanishing points from its manually measured true position is five pixels, (the true position was decided by using

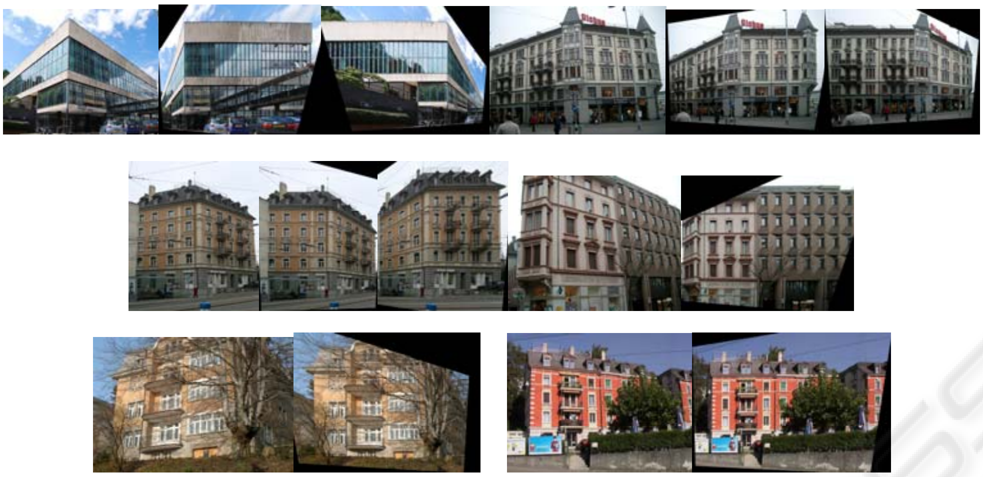

Figure 5: Some example images with their associated warped facades.

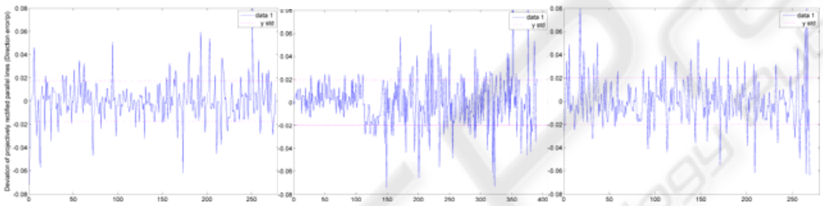

Figure 6: Deviation errors from being parallel of the projective warped lines (for first three building examples in Fig.5) – assessing vanishing point accuracy in each line set.

ruler to extend major building lines and locating the intersection).

(2) Better Grouping of Lines. Buildings can have facades which do not necessarily align with the three orthogonal axes as shown in Fig. 4(a). Images of buildings can also be taken from a critical viewpoint where false initial groupings occur (Fig. 4(d)). The problem of false grouping can also easily occur when the vanishing points' initial position is decided by the intersection of lines with similar orientations. The refinement method solved this by iteratively adjusting the position of the vanishing points and line groupings.

(3) Adaptable to Occlusion, Illumination and Viewpoint Change. These factors need to be considered when dealing with building images. Fig. 5 shows some of the rectified building facades using the proposed method that have been successfully adapted. At the rectification stage, the accuracy of each vanishing point obtained with the final grouped line segments in each vanishing direction set can be also assessed by investigating parallel lines after applying the projective transformation **P**. In theory, the projective matrix **P** can recover the lines to affinity. This means that the line direction in each group should be the same. From the experiment, the average deviation error was 1.8%. Fig. 6 shows the plots of parallel deviation errors for the first three building example of Fig. 5. In addition, instead of directly applying computed projective, affine and similarity transformations to the original image, the three-stage transformations were only applied to grouped line sets. After the final transformation, three least-deviating (from parallel to x or y axis) line segments were selected for final image registration in order to reduce rectification distortion introduced by lines with large deviation errors.

4 CONCLUSIONS

In conclusion, our approach for building facade rectification is generally robust to occlusions, different illuminations, wide changes in viewpoint and different camera settings. The method could be improved further by analysing the peaks detected at the stage of curve fitting. For example, instead of selecting the highest two or three peaks for grouping, minor peaks could also be included. Groups with similar initial estimates could be combined at the refinement stage. This kind of improvement can also enable rectification of a collection of buildings appeared in a single image.

REFERENCES

Chen, Y & Ip, H, H, S 2005, 'Planar metric rectification by algebraically estimating the image of the absolute conic', In *Proc IEEE conf. on Pattern Recognition*, vol. 38, pp. 1117-1120.

David, P 2008, 'Detection of building facades in urban environments', In *Proc. SPIE conf. on Visual Information Processing XV!!,* vol. 6978, pp. 9780-9780.

Hartley, R, I 1999. 'Theory and practice of projective rectification', *International Journal of Computer Vision*, vol. 35, pp. 115-127.

Hu, J, Sawyer, J & Herve, J, Y 2006, 'Building detection and recognition for an automated tour guide', In *Proc. IEEE Conf. on Systems, Man and Cybernetics*, vol. 1, pp. 283-289.

Košecká, J & Zhang, W 2002, 'Video compass', In *Computer Vision — ECCV,* vol. 2353, pp. 29-32.

Košecká, J & Zhang, W 2005, 'Extraction, matching, and pose recovery based on dominant rectangular structures', *Computer Vision and Image Understanding*, vol. 100, pp. 274-293.

Liebowitz, D & Zisserman, A 1998, 'Metric rectification for perspective images of planes', In *Proc. IEEE Conf. on Computer Vision and Pattern Recognition*, pp. 482-488.

Menudet, J, F, Becker, J, M, Fournel, T & Mennessier, C 2008, 'Plane-based camera self-calibration by metric rectification of images', *Image and Vision Computing*, vol. 26, pp. 913-934.

Robertson, D & Cipolla, R 2004. 'An image-based system for urban navigation', In *Proc. British Machine Vision Conference*.

Wang, G, Hu, Z, Wu, F & Tsui, H, T 2005, 'Single view metrology from scene constraints', *Image and Vision Computing*, vol. 23, pp. 831-840.

Kovesi, P 2000-2006, http://www.csse.uwa.edu.au/~pk/research/matlabfns/

Shao, T, S, H & Gool, L, V (2003), 'Zubud-zurich buildings database for image based recognition', *Technical report No. 260*, Swiss Federal Institute of Technology, http://www.vision.ee.ethz.ch/showroom/zubud/

Hartley, R, & Zisserman, A 2003, *Multiple View Geometry in Computer Vision*, Cambridge University Press, Second Edition, Chapter 8.